

The angular correlation between the fission fragment intrinsic spins

Aurel Bulgac^{1, *}

¹*Department of Physics, University of Washington, Seattle, Washington 98195–1560, USA*

(Dated: August 2, 2022)

The generation of fission fragments (FF) spins and of their relative orbital angular momentum has been debated for more than six decades and no consensus has been yet achieved so far. The interpretation of recent experimental results of Wilson *et al.* [Nature, **590**, 566 (2021)] have been challenged by several recent theoretical studies, which are not in agreement with one another. According to Wilson *et al.*'s interpretation [Nature, **590**, 566 (2021)], the FFs spins emerge very long after scission occurred. Randrup and Vogt [Phys. Rev. Lett. **127**, 062502 (2021)], while agreeing that the FF spins are uncorrelated, conclude on the basis of a phenomenological model that these spins are uncorrelated already before scission. Bulgac *et al.* [Phys. Rev. Lett. **128**, 022501 (2022)] in a fully microscopic study demonstrate that the primordial FF spins final values are defined before the emission of prompt neutrons and statistical gammas and are strongly correlated with a relative angle between spins close to $2\pi/3$, a result in full agreement with the present independent analysis. The prompt neutrons and statistical gammas carry a significant amount of angular momentum according to the study of Stetcu *et al.* [Phys. Rev. Lett. **127**, 222502 (2021)], which can lead to a decorrelation of the FF bandhead spins of the yrast lines measured by Wilson *et al.* [Nature, **590**, 566 (2021)], and which also provides arguments why these measured spins are so different from the primordial FF spins evaluated by Bulgac *et al.* [Phys. Rev. Lett. **128**, 022501 (2022)]. Here, I show that the unexpected character of the angular correlation between the primordial FF intrinsic spins, recently evaluated by Bulgac *et al.* [Phys. Rev. Lett. **128**, 022501 (2022)], which favors FF intrinsic spins pointing predominantly in opposite directions, can be understood by using simple general phase space arguments. The observation by Wilson *et al.* [Nature, **590**, 566 (2021)] that the FF spins are uncorrelated follows from both the results of the microscopic calculation of Bulgac *et al.* [Phys. Rev. Lett. **128**, 022501 (2022)] and the present analysis of the full correlated probability distribution of the FF spins together with the relative orbital angular momentum of the primordial FFs. These arguments may apply also to heavy-ion collisions and since there is no use of specifics of the particle interactions, the present results might apply to atomic and molecular systems as well.

I. INTRODUCTION

The origin and the dynamics of the fission fragments (FFs) intrinsic spins and of their relative orbital angular momentum between the FFs are topics with a very long history and many unsettled and conflicting interpretations and claims, see a representative, but definitely not complete, list of references [1–23]. The results of the complex microscopic simulations performed in Ref. [22] proved to be an unexpected surprise, at odds both with the interpretation by Wilson *et al.* [19] of their experimental data, and also at odds with a recent study performed by Vogt and Randrup [17] and Randrup and Vogt [18] within the framework of the phenomenological model FREYA. Moreover, while Randrup and Vogt [18] agree with Wilson *et al.* [19] that the FF intrinsic spins are at most weakly correlated, in their analysis these FF spins emerge almost uncorrelated *before scission*, while the assumed nucleon-exchange mechanism between the preformed FFs is at work [24, 25]. Thus, the analysis of Randrup and Vogt [18] invalidates the interpretation of Wilson *et al.* [19] of their own experimental results, who state that the FF spins emerge uncorrelated *after scission*, a claim which cannot be reconciled with any

conceivable theoretical dynamic model. In a subsequent study within the Hauser-Feshbach framework [26], Stetcu *et al.* [23], demonstrate that after scission, the highly excited primordial FFs emit prompt neutrons and statistical gammas, which carry a significant amount of angular momentum, $\approx 3.5 - 5\hbar$. These results can explain the observed values of the yrast bandheads measured by Wilson *et al.* [19] and also why these FF spins might appear uncorrelated at that point in the fission dynamics.

Here I will present a transparent analysis of the unexpected theoretical prediction presented recently in Ref. [22], namely that the directions of the primary FF intrinsic spins are strongly correlated, in a manner not inferred from previous studies, either experimental, phenomenological, or microscopic. One can suspect that the complexity of the implementation of the Time-Dependent Density Functional Theory (TDDFT) [27–30] could contain some unidentified errors and subsequently lead to an erroneous conclusion in Ref. [22]. The uncertainties of the nuclear energy density functionals (NEDF) [31] or complexity of the TDDFT numerical implementation could hide some erroneous inputs. One can also speculate that long memory effects [32, 33] are relevant when the collective velocities of the fission dynamics are even slower than in the adiabatic approximation [29, 30]. On the other hand phenomenological models typically rely on a large number of parameters and nuclear properties, many of them not known with sufficient precision, if at

* bulgac@uw.edu

all. As the recent microscopic studies have shown [20–22], phenomenological studies [17, 34–38] assume incorrectly that the moment of inertia of the heavy (H) FF is larger than that of the light (L) FF, an aspect corrected in Ref. [18], where an *ad hoc* phenomenological parametrization of the FF moments of inertia was introduced. Microscopic studies [29, 30] also clearly demonstrate that the FF temperatures are different and typically the heavy FF has less excitation energy than the light FF, an aspect neglected in the FREYE model [17, 18]. The interpretation of the experimental results of Wilson *et al.* [19] and the recent conflicting theoretical and phenomenological conclusions [17, 18, 20–23], and also the range of conflicting initial assumptions in these approaches, might fail to convince the wider audience of their reliability and can greatly benefit from an independent analysis.

II. THEORETICAL APPROACH

The theoretical framework adopted here has similarities with the Fermi’s golden rule derivation, where the transition probability per unit time from an initial state to all allowed by conservation laws final states, is the product between the square of an average matrix element, often taken as a phenomenological constant, and the density of the final states, which can be often easily evaluated. A particular pedagogical example of the use of the Golden rule is that of the rate of the neutron β -decay, which shows that the shape of the electron spectrum is fully determined by the density of final states and the energy, momentum, and angular momentum conservation laws.

One can define the angle between the FF intrinsic spins,

$$\phi^{LH} = \left\langle \arccos \frac{\mathbf{S}^L \cdot \mathbf{S}^H}{S^L S^H} \right\rangle, \quad (1)$$

where the brackets $\langle \rangle$ stand for the quantum mechanical expectation value of this complex operator. I will show that in the case of FF intrinsic spins, the shape of the distribution $p(\phi^{LH})$ is controlled by the structure of the available phase space of the final FF intrinsic spins and their relative orbital angular momentum, and that this distribution is only weakly dependent on the fission mechanism.

The only input needed in the present analysis will be the quantum theory of angular momentum and only some very mild and quite general and flexible assumptions about the individual angular momentum distributions. Since all relative FF intrinsic spin degrees of freedom, bending and wriggling, twisting and tilting, are treated explicitly, the present analysis is more general than the microscopic treatment presented in Ref. [22] and FREYA [17, 18], where only the bending and wriggling modes were explicitly considered.

I will limit at first the analysis to the very clean case of the spontaneous fission of an even-even nucleus, such as

$^{252}\text{Cf}(\text{sf})$, which has an initial spin and parity $S_0^\pi = 0^+$. In this case the two FF intrinsic spins $\mathbf{S}^{L,H}$ and their relative orbital angular momentum $\mathbf{\Lambda}$ satisfy the relation

$$\langle \mathbf{S}_0 \rangle = \langle \mathbf{S}^L + \mathbf{S}^H + \mathbf{\Lambda} \rangle = \mathbf{0}, \quad (2)$$

and where by definition Λ is an integer. In the classical limit all three components of each of these angular momenta have well defined values. In this limit these three vectors lie in a plane and $\mathbf{\Lambda}$ is perpendicular to the fission direction. The FF intrinsic spins $\mathbf{S}^{L,H}$ are not restricted to lie in a plane perpendicular to the fission direction in the present analysis, unless the FFs emerge only with $K^{L,H} = 0$ projections of their respective intrinsic spins. At the quantum mechanical level only the magnitude and one cartesian component of each angular momentum can have simultaneously well-defined values. Quantum fluctuations therefore lead to “fluctuations” of the orientation of the plane formed by these three vectors. Before scission the identity of the FFs is not uniquely defined, as matter, momentum, angular momentum, and energy is flowing between them. The FF intrinsic spins and $\mathbf{\Lambda}$ are well-defined only at a sufficiently large separation between FFs, albeit for the role of the long-ranged Coulomb interaction [39, 40] and the presentations of Bertsch, Scamps, Bulgac at the recent *Workshop on Fission Fragment Angular Momenta* [41].

Since the average values of these three angular momenta are $\mathcal{O}(10\hbar)$ [17, 18, 20–23] in the following discussion I will use often a classical interpretation of the angular momenta. Eq. (2) implies that out of the 9 Cartesian components of these angular momenta only 6 are independent and I choose the triangle formed by them to lie in the Oxy -plane and the vector $\mathbf{\Lambda}$ to be along the Ox -axis. In that case Eq. (2) can be re-written explicitly as

$$S_x^L + S_x^H = -\Lambda, \quad (3a)$$

$$S_y^L = -S_y^H, \quad (3b)$$

$$S_z^L = S_z^H = 0, \quad (3c)$$

and thus only 3 cartesian components are then left independent. The fission direction then lies in the Oyz -plane.

I will choose the magnitudes of these angular momenta Λ and $S^F = \sqrt{(S_x^F)^2 + (S_y^F)^2}$ as variables in the following analysis. The magnitudes of these angular momenta satisfy the triangle restriction

$$|S^L - S^H| \leq \Lambda \leq S^L + S^H. \quad (4)$$

I will assume that there is an upper momentum cutoff S_{max} for $S^{L,H}$, which can be taken to infinity if ever needed. FFs can be odd or odd-odd nuclei, and in the case of odd FFs the intrinsic spin is a half-integer. I ignore this possibility here, which however is trivial to include and does not affect the conclusions. It is easy to see that the number of points in the 3-dimensional space consistent with this maximum angular momentum

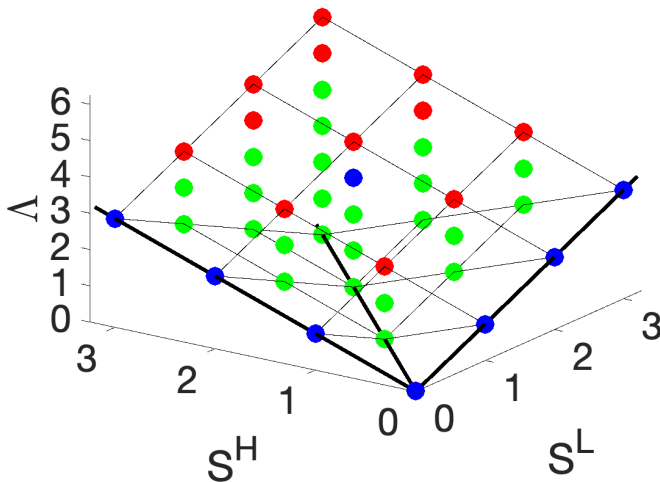


FIG. 1. In this figure the bullets fill out a three face pyramid with the apex at $(0, 0, 0)$. The green bullets show the triplets (S^L, S^H, Λ) for which $\cos \phi^{LH} < 0$, the blue bullets for $\cos \phi^{LH} = 0$, and the red bullets for $\cos \phi^{LH} > 0$, when $S_{\max} = 3$. The green bullets correspond to $\phi^{LH} > \pi/2$ and the red bullets correspond to $\phi^{LH} < \pi/2$. The ratio of red to green bullets for any S_{\max} value is always close to 0.5, which means that the number of configuration in which the FF intrinsic spins point in opposite direction is dominant. The black lines are the intersection of the pairs of planes $(S^L = S^H, \Lambda = 0)$, $(S^L = \Lambda, S^H = 0)$, $(S^H = \Lambda, S^L = 0)$ respectively and they cross at $(0, 0, 0)$. The points on each face are joined by thin lines.

is $(2S_{\max} + 1)(S_{\max} + 1)^2$. At the same time, the triangle constraint (4) allows only for about 1/3 of the total number of configurations, more exactly for

$$N_0 = \frac{2}{3}(S_{\max} + 1)^3 + \frac{1}{3}(S_{\max} + 1) \approx \frac{2}{3}S_{\max}^3. \quad (5)$$

In Fig. 1 I plot the distribution of the allowed values of the triplet (S^L, S^H, Λ) for a small value of $S_{\max} = 5$. The allowed angular momenta $S^{L,R}$ and Λ are in the interior of a three faced pyramid defined by the planes

$$+\Lambda - S^L - S^H = 0, \quad (6a)$$

$$-\Lambda + S^L - S^H = 0, \quad (6b)$$

$$-\Lambda - S^L + S^H = 0. \quad (6c)$$

The number of triplets (S^L, S^H, Λ) corresponding to $\phi^{LH} > \pi/2$ (green bullets) is about twice as large than the number of points corresponding to $\phi^{LH} < \pi/2$ (red bullets) for any value of S_{\max} and that is the main reason why the angles $\phi^{LH} > \pi/2$ between the two FF spins are favored. In the limit $S_{\max} \rightarrow \infty$ a fraction 0.65 of the pyramid volume corresponds to $\phi^{LH} > \pi/2$ and there only less than a quarter of the allowed values for these angular momenta correspond to angles $\phi^{LH} < \pi/2$.

There is another very simply qualitative argument on why the angle between the two FF intrinsic spins is larger

than $\pi/2$. The three spins $S^{L,H}$ and Λ can be arranged tail to tail to form a “Mercedes”-like star. The triangle constraint (4) is fully symmetric with respect to any permutation of the three angular momenta and can be re-written in two other equivalent forms

$$|S^L - \Lambda| \leq S^H \leq S^L + \Lambda, \quad (7a)$$

$$|S^H - \Lambda| \leq S^L \leq S^H + \Lambda, \quad (7b)$$

as it is clear as well from Eqs. (6). There is no preferential role for Λ and on average the angle between any two angular momenta is naturally $2\pi/3$ for any random arrangement of them, if all three angular momenta are generated with identical distributions.

The arguments presented above refer only to the structure of the FF intrinsic spin final configurations, when all three spins add to zero and make no reference to possible role of the dynamics and in this sense this argument is similar to the one used in deriving the Fermi’s golden rule.

The next step is to generate distributions of these FF intrinsic spins and orbital angular momentum consistent with Eq. (4) and their form depends on the nucleon interactions. I will consider here at first two types of spin distributions, namely a uniform distribution

$$P_1(S^{L,H}) = \frac{1}{S_{\max}}, \quad P_1(\Lambda) = \frac{1}{2S_{\max}}, \quad (8)$$

which implies total ignorance about the angular momenta and a statistical distribution, derived in the Fermi gas model by Bethe in 1936 [2, 42]

$$P_1(S^{L,H}) \propto (2S^{L,H} + 1) \exp \left[-\frac{S^{L,H}(S^{L,H} + 1)}{2\sigma^{L,H}} \right], \quad (9a)$$

$$P_1(\Lambda) \propto (2\Lambda + 1) \exp \left[-\frac{\Lambda(\Lambda + 1)}{2\sigma^\Lambda} \right]. \quad (9b)$$

The experience accumulated since 1936 is that a statistical distribution based on the Fermi gas model is quite close to reality, if one neglects quantum or shell effects. Here, the parameters $\sigma^{L,H}$ and σ^Λ are chosen so as to reproduce approximately the corresponding FF intrinsic spins distributions determined in microscopic simulations [20, 22]. Bethe’s approximation of a Fermi gas distribution seems quite reasonable, apart from shell-corrections, as nucleons move predominantly in a mean field, and level density and spin distributions are thus quite reasonable. However, one cannot make the same argument concerning $P_1(\Lambda)$. The ansatz

$$P(\Lambda) \propto \sum_{S^{L,H}} P_1(S^L)P_1(S^H)\Delta \quad (10)$$

with $P_1(S^{L,H})$ from Eq. (9a) and where Δ

$$\Delta = \Theta(\Lambda - S^L - S^H)\Theta(|S^L - S^H| - \Lambda) \quad (11)$$

with $\Theta(x) = 1$ if $x \geq 0$ and $\Theta(x) = 0$ if $x < 0$ is enforcing the triangle rule, see Eqs. (4), leads to a distribution

$P(\Lambda)$ very similar to Eq. (9b). See also the discussion below and later on see Eqs. (27), (29) and Fig. 3, for a different choice for $P(\Lambda)$ suggested by Thomas Dossing at the recent *Workshop on Fission Fragment Angular Momenta* [41].

From such individual FF intrinsic spins and orbital angular momentum distributions I generate the combined distributions

$$\bar{P}_3(S^L, S^H, \Lambda) = \mathcal{N} P_1(S^L) P_1(S^H) P_1(\Lambda) \Delta, \quad (12)$$

where

$$\sum_{S^L, S^H, \Lambda} \bar{P}_3(S^L, S^H, \Lambda) = 1, \quad (13)$$

and where \mathcal{N} is an appropriate normalization factor. Alternatively, one can use also $P_1(\Lambda)$ from Eq. (10) with little changes in the final results. This combined distribution $\bar{P}_3(S^L, S^H, \Lambda)$ vanishes outside the region defined by Eq. (4) in the 3-dimensional space (S^L, S^H, Λ) and it allows for the presence of the twisting and tilting modes.

In the simulations each of the FF intrinsic spins and of the orbital relative angular momentum populate large angular momentum intervals. It is important to recognize that Eq. (4) implies that the support of these distributions cannot be drastically different, as otherwise Eqs. (4, 7) cannot be satisfied. If one of these distributions, e.g. $P_1(\Lambda)$, is very wide, while the other two are much narrower, the triangle constraint can be satisfied only for relatively small values of the angular momenta Λ , and the longer tails of $P_1(\Lambda)$ will never contribute to any physical situation, see also the discussion below. Therefore, such drastically different angular momentum distribution cannot emerge from any realistic calculations, where rotational symmetry is satisfied.

In this work I determine the probability distribution $p(\phi^{LH})$, $\int_0^\pi d\phi^{LH} p(\phi^{LH}) = 1$, where ϕ^{LH} is the angle between S^L and S^H by constructing a histogram of the expectation of the cosine between them

$$\cos \phi^{LH} = \frac{\Lambda(\Lambda + 1) - S^L(S^L + 1) - S^H(S^H + 1)}{2(S^L + 1/2)(S^H + 1/2)}. \quad (14)$$

The magnitudes of the 3 angular momenta are expressed in units of \hbar and I will use the units $\hbar = 1$ henceforth. In the denominator of Eq. (14) I introduced the well known Langer correction [43] to the FF intrinsic spins, which is not needed in the numerator. Eq. (14) can be readily derived from Eq. (2) by replacing the scalar product with

$$\mathbf{S}^L \cdot \mathbf{S}^H \rightarrow (S^L + 1/2)(S^H + 1/2) \cos \phi^{LH}. \quad (15)$$

The angle ϕ^{LH} depends only on the shape of the triangle, or the shape of the ‘‘Mercedes-star’’ the three angular momenta form, but not on its spatial size nor on its particular orientation in space. The only relevant dimensional scale, \hbar , vanishes in the classical limit and as a result all quantities $\mathcal{O}(1)$ should be neglected in this limit, e.g. 1/2 and 1 in Eq. (14).

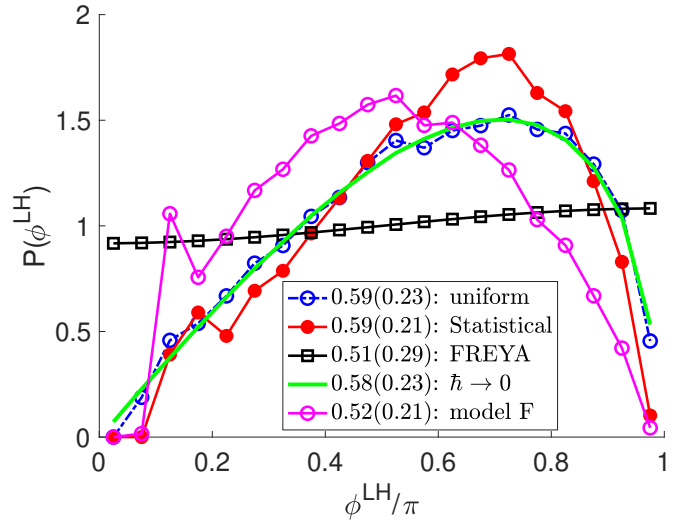


FIG. 2. The uniform angular momentum distribution (8) was obtained with an $S_{\max} = 30$, see Eq. (8), and represented here as a histogram with 20 bins. The statistical distribution was obtained with $\sigma^L = 108.2$, $\sigma^H = 44.8$ and $\sigma^\Lambda = 161.3$, which closely reproduce the corresponding distributions obtained in Refs. [20, 22] for ^{240}Pu . The FREYA distribution was obtained with typical parameters from [17, 18]. The $\hbar \rightarrow 0$ classical limit was obtained by taking $S_{\max} \rightarrow \infty$ for the uniform distribution. The results obtained with a modified FREYA prescription $P_{\text{model F}}$ introduced here are shown with magenta circles. The average and variance (in parentheses) of ϕ^{LH}/π for each distribution are displayed next to each label. The lines connecting the markers are only for guiding the eye. For visual purposes the distribution displayed here differs by a factor from Eq. (16), $P(\phi^{LH}) = \pi p(\phi^{LH})$. The FREYA results from Ref. [18] and reproduced here are markedly different from the distributions derived here and from the microscopically evaluated distribution $p(\phi^{LH})$ in Ref. [22]. In the space (S^L, S^H, Λ) the allowed configurations with $\phi^{LH} = \pi$ correspond to the lateral lower faces of the pyramid in Fig. 1, see Eqs. (6b, 6c), when $\Lambda = |S^L - S^H|$. The allowed configurations with $\phi^{LH} = 0$ correspond to upper face of the pyramid $\Lambda = S^L + S^H$ in Fig. 1, see Eq. (6a). All faces have dimension 2, as opposed to the dimension 3 of the space of the rest of allowed configurations (S^L, S^H, Λ) , which makes obvious the presence of the strong suppression at $\phi^{LH} = 0, \pi$. This clear discrepancy between the predictions made in Refs. [17, 18] and reproduced here and the predictions made in the present work and in Ref. [22] remains to be resolved in future experiments, see also Sobotka’s talk at the *Workshop of Fission Fragment Angular Momenta* [41].

I generate all N_0 , see Eq. (5), triplet configurations (S^L, S^H, Λ) allowed by Eq. (4) and each such configuration is weighted with probability $\bar{P}_3(S^L, S^H, \Lambda)$ (12). Then the probability distribution $p(\phi^{LH})$ is constructed

as follows

$$p(\phi^{LH}) = \sum_{S^L, S^H, \Lambda} \bar{P}_3(S^L, S^H, \Lambda) \delta_{\psi(S^L, S^H, \Lambda), \phi^{LH}}, \quad (16)$$

$$\sum_{\phi^{LH}=0}^{\phi^{LH}=\pi} p(\phi^{LH}) = 1, \quad (17)$$

$$\psi(S^L, S^H, \Lambda) = \arccos \left[\frac{\Lambda(\Lambda + 1) - S^L(S^L + 1) - S^H(S^H + 1)}{2(S^L + 1/2)(S^H + 1/2)} \right], \quad (18)$$

where $\delta_{\psi, \phi} = 1$ if $\phi = \psi$ and zero otherwise, is the Kronecker symbol and the values $\psi(S^L, S^H, \Lambda)$ are discrete. Thus $p(\phi^{LH})$ represents a discrete point with coordinates $(\phi^{LH}, p(\phi^{LH}))$. For each triplet (S^L, S^H, Λ) the corresponding angle $\psi(S^L, S^H, \Lambda)$ is weighted with probability $\bar{P}_3(S^L, S^H, \Lambda)$ and its contribution is added to the corresponding ϕ^{LH} -bin in Fig. 2.

In Fig. 2 I show five distributions for $p(\phi^{LH})$ obtained by using the uniform distributions Eq. (8) (blue circles), the statistical distributions Eqs. (9) (red bullets), the distribution predicted by the FREYA model [17, 18] (black squares), the limiting classical distribution ($\hbar \rightarrow 0$) obtained by taking the limit $S_{\max} \rightarrow \infty$ (green line) for a uniform distribution, and a model F distribution inspired by FREYA, which is discussed below.

In the classical limit one can eliminate the angular momenta lengths and introduce their relative normalized lengths

$$s^L + s^H + \lambda = 1, \quad (19)$$

$$\psi(s^L, s^H, \lambda) = \arccos \frac{\lambda^2 - (s^L)^2 - (s^H)^2}{2s^L s^H}, \quad (20)$$

and the distribution $p(\phi^{LH})$ can be evaluated from

$$p(\phi^{LH}) = 3 \int_0^1 ds^L \int_0^{s^L} ds^H \int_{s^L - s^H}^{s^L + s^H} d\lambda \quad (21)$$

$$\times \delta[\phi^{LH} - \psi(s^L, s^H, \lambda)],$$

when all shapes are equiprobable (uniform distributions).

The uncanny similarity to the distribution $p(\phi^{LH})$ reported in Ref. [22] is striking. The distributions in Fig. 2 were obtained without any input from the dynamics, unlike the results of Ref. [22]. By changing the form of the individual distributions $P_1(S^L)P_1(S^H)P_1(\Lambda)$ the final aspect of $p(\phi^{LH})$ changes very little from the uniform to the statistical distribution. In the classical limit, which can be achieved either for very large momenta or very high temperatures, the distribution becomes very smooth (no quantum or “shell-like corrections”), as expected. The triangle constraints (4, 7) which enforce the conservation of the total angular momentum of the entire nuclear systems leads to strongly correlated FF intrinsic spins, as it is clear from Fig. 2, with some weak “shell correction.” As in the case of Bethe level density, the role of the

nucleon interactions is relatively small. The uniform angular momenta distributions (8), the statistical distributions Eqs. (9), and the classical limit (21), are rather close to each other. This implies that the primary FF intrinsic spins form preferentially and angle larger than $\pi/2$ (similarly to any two prongs of a “Mercedes-star”), thus favoring the bending modes over the wriggling modes. There are no qualitative changes when different distributions, because the number of configurations with $\phi^{LH} > \pi/2$ is always about twice as big as the number of configurations with $\phi^{LH} < \pi/2$, see Fig. 1, which is the defining feature of this distribution. With increasing temperature, or equivalently, in the classical limit, the size of the triangles increases, but the shape remains the same, and the $p(\phi^{LH})$ changes relatively little, apart from the diminishing role of the $\mathcal{O}(\hbar)$ corrections, as expected on general grounds. The fact that one does not see a perfect agreement with the simple geometrical arguments presented above, when the expected angle between any two angular momenta is $2\pi/3$, is due to the fact that the widths of the $P_1(S^{L,H})$ and $P_1(\Lambda)$ are different and the full permutation symmetry between all these angular momenta is slightly broken. In particular, in fission this symmetry is broken by the mass and deformation differences between the heavy and light FFs.

One can change the character of this FF intrinsic spins distribution only by choosing a distribution of angular momenta $\bar{P}_3(S^L, S^H, \Lambda)$, which drastically favors angles $\phi^{LH} < \pi/2$, for example choosing a distribution $P_1(\Lambda)$ which favors $S_{\max} \leq \Lambda \leq 2S_{\max}$. In such a situation the two FFs emerge at scission as a system similar to a planet and its moon of comparable mass, rotating around their common center-of-mass with a quite high frequency and predominantly parallel spins. In such a case the probability distribution $p(\phi^{LH})$ will favor angles $\phi^{LH} < \pi/2$ and the tilting and wriggling modes will be the dominant ones, as opposed to the twisting and bending modes otherwise. One can imagine such a quasi-fission process in a heavy-ion collision with a relatively large initial spin S_0 of the compound nucleus. Since the initial spin of the compound nucleus is now $S_0 \neq 0$ one has to discuss instead the probability distribution $\bar{P}_3(S^L, S^H, |\Lambda - \mathbf{S}_0|)$, which will proceed along the same lines as above.

The distributions discussed here have a very distinct fingerprint, they vanish in the classical limit at $\phi^{LH} = 0$ and π , which happens in Fig. 1 on the faces of the three face pyramid, where the allowed phase space is restricted to a 2D region. This feature is absent in FREYA results [17, 18].

In FREYA the rotational energy, which controls the spin distributions, has the form [17, 18]

$$E_{\text{rot}} = \frac{\mathbf{S}^L \cdot \mathbf{S}^L}{2I^L} + \frac{\mathbf{S}^H \cdot \mathbf{S}^H}{2I^H} + \frac{\mathbf{\Lambda} \cdot \mathbf{\Lambda}}{2I^R}, \quad (22)$$

with the moments of inertia $I^R \gg I^{L,H}$. This distribution can be used in a statistical description where T is a phenomenological temperature of the fissioning nucleus

and Z an appropriate normalization factor.

$$\begin{aligned} P(S^L, S^H, \Lambda) &= \frac{1}{Z} \exp \left[-\frac{E_{\text{rot}}}{T} \right], \\ &= P_1(S^L) P_1(S^H) P_1(\Lambda). \end{aligned} \quad (23)$$

This formula assumes that all these momenta can change only by interacting with the rest of the degrees of freedom, which play the role of a thermal bath, which equally implies that the two FFs are still in contact with each other. Microscopic studies show [29, 30] that the FFs have however different temperatures and it is unclear how a temperature for Λ can be defined then. While this ansatz for E_{rot} (22) appears as a natural starting point [9, 12], it does not have the most general form allowed by rotational symmetry. The assumption that the FF shapes and their relative orientations do not play any role in their dynamics appears to be very unlikely, see some of the arguments presented by Bulgac, Bertsch and Scamps at the recent *Workshop on Fission Fragment Angular Momenta* [41] and Ref. [40]. Assuming that one can limit the description of the rotation dynamics to these three angular momenta alone, after eliminating all the relevant angles, the most general form allowed by symmetry for the rotational energy is

$$E_{\text{rot}} = (\mathbf{S}^L, \mathbf{S}^H, \mathbf{\Lambda})^T \otimes \overset{\leftrightarrow}{\mathbf{I}} \otimes (\mathbf{S}^L, \mathbf{S}^H, \mathbf{\Lambda}), \quad (24)$$

with a non-diagonal 3×3 inertia tensor $\overset{\leftrightarrow}{\mathbf{I}}$ in general, see also Ref. [22]. A very simple analog is the effective position dependent nucleon mass in mean field approaches, which in principle can become a tensor as well [44], and also the numerous examples Brillouin zones with strongly anisotropic electron kinetic energy dispersion.

With no triangle constraints (4, 7) and no intrinsic spins correlation Eq. (23) implies $\langle \mathbf{S}^L \cdot \mathbf{S}^H \rangle \equiv 0$. Following the framework described above I introduce instead a distribution inspired by FREYA

$$P_{\text{model F}}(S^L, S^H, \Lambda) = \mathcal{N} \exp \left[-\frac{E_{\text{rot}}}{T} \right] \Delta \quad (25)$$

where \mathcal{N} is an appropriate normalization factor and using Eq. (22). This distribution is more general than the one used in the FREYA phenomenological model, as it allows also for the tilting and twisting degrees of freedom to be taken into account, and moreover at the quantum level. Even though this $P_{\text{model F}}(S^L, S^H, \Lambda)$ depends on the initially very wide distribution $P_1(\Lambda)$, see Eq. (23) with E_{rot} from Eq. (22), the triangle constraint and the subsequent renormalization lead to a physically acceptable distribution, with a physically acceptable average $\langle \Lambda \rangle$ and variance/cumulant $\langle \langle \Lambda^2 \rangle \rangle$, due to similar arguments presented in connection with Eq. (10). In the limit of infinite temperature the distribution $p(\phi^{LH})$ is expected to become very smooth (no quantum or ‘‘shell corrections’’) similar to the classical distribution shown with a green line in Fig. 2, for either the uniform (8) or the statistical distributions (9), where I used $S_{\text{max}} = 200$.

One can visually see a relatively small preponderance of angles $\phi^{LH} > \pi/2$, as expected. With increasing temperature for this model F distribution the average and variance of the angle ϕ^{HL} does not change significantly if $I^{\text{R}} \gg I^{L,H}$.

In FREYA [17, 18] the non-conservation of the total angular momentum due to the presence of a thermal bath of the probability distribution (23) is resolved by imposing the additional constraint $\Lambda = |\mathbf{S}^L + \mathbf{S}^H|$. All the angular momenta are treated classically $\mathbf{S}^{L,H} \cdot \mathbf{S}^{L,H} = (S^{L,H})^2$ and the tilting and twisting intrinsic spin degrees of freedom (the FF rotations around the fission axis) are assumed to be suppressed [10, 17]. With increasing temperature the angular momenta increase in size $\propto \sqrt{T}$ and since the geometry of the triangle (4) is the same at all temperatures, the FREYA prediction [17, 18] for $p(\phi^{LH})$ is independent of temperature and FREYA framework and it is technically a high-temperature limit of the quantum distribution. The primordial FF intrinsic spin correlations arise from the orbital rotational energy term, see Eq. (22), only after the replacement

$$\frac{\mathbf{\Lambda} \cdot \mathbf{\Lambda}}{2I^{\text{R}}} \rightarrow \frac{\mathbf{S}^L \cdot \mathbf{S}^L}{2I^{\text{R}}} + \frac{\mathbf{S}^H \cdot \mathbf{S}^H}{2I^{\text{R}}} + \frac{\mathbf{S}^L \cdot \mathbf{S}^H}{I^{\text{R}}}, \quad (26)$$

and specifically from the last term in this relation with $I^{\text{R}} \approx 10I^{L,H}$, which leads to very weak antiparallel FF intrinsic spins correlations, at the level of $\approx 10\%$, see Fig. 2 and Refs. [17, 18]. An almost uniform $p(\phi^{LH})$ distribution as predicted by FREYA can be obtained in the unlikely case when the correlated distribution $P_3(S^L, S^H, \Lambda)$ diverges for $\Lambda = |\mathbf{S}^L \pm \mathbf{S}^H|$, see Appendix.

During the recent *Workshop of Fission Fragment Angular Momenta* [41] the character of the distribution $p(\phi^{LH})$ was extensively discussed, see in particular the slides and the video recordings of the talks given by Randrup, Vogt, Bulgac (2), Dossing and Sobotka. Thomas Dossing suggested an alternative parametrization of the probability distribution $\tilde{P}_3(S^L, S^H, \Lambda)$

$$\begin{aligned} \tilde{P}_3(S^L, S^H, \Lambda) &= \mathcal{N} P_1(S^L) P_1(S^H) \\ &\times \left[C_{S^L,0,S^H,0}^{\Lambda,0} \right]^2 \exp \left[-\frac{\Lambda(\Lambda+1)}{2I_{\text{rel}}T} \right], \end{aligned} \quad (27)$$

where \mathcal{N} is an appropriate normalization constant and $C_{S^L,0,S^H,0}^{\Lambda,0}$ are Clebsch-Gordan coefficients. This distribution $\tilde{P}_3(S^L, S^H, \Lambda)$ assumes that the primordial FF intrinsic spins, before the emission of prompt neutrons and statistical γ -rays are strictly perpendicular to the fission axis ($K^{L,H} = 0$), thus allowing only for the bending and wriggling modes of FF intrinsic spins, similarly to what it is assumed in FREYA [17, 18]. In the analysis of this probability distribution I have used the exact values of the Clebsch-Gordan coefficients [45]. It also assumes that the relative orbital angular momentum is thermalized to the same temperature as the FF intrinsic spins. Randrup in his presentation at the *Workshop of Fission Fragment Angular Momenta* [41] stressed that FREYA can be also

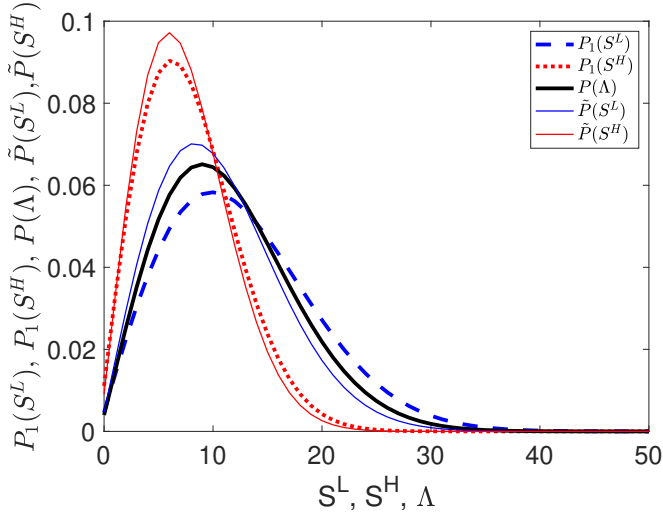


FIG. 3. The distributions $P_1(S^{L,H})$ (9a) along with the distributions $\tilde{P}(S^{L,H})$ and $P(\Lambda)$, see Eqs. (28, 29) obtained from distribution $\tilde{P}_3(S^L, S^H, \Lambda)$ (27) by summing over the rest of angular momenta, are shown for ^{252}Cf . The FF intrinsic spin distributions $P_1(S^F) \approx \tilde{P}(S^F)$ and the relative orbital angular momentum distribution $P(\Lambda)$ obtained from Eq. (29) is very similar in shape to the statistical distribution $P_1(\Lambda)$ from Eq. (9b).

used with different temperatures for different rotational modes (wriggling, bending, and maybe twisting, which is typically neglected). Here I_{rel} was chosen as the relative moment of inertia of two touching rigid sphere with the average mass close to the average fission yields for induced fission of ^{240}Pu and $T = 1$ MeV. A fairly similar distribution is obtained for either $T = 0.75$ or 0.5 MeV temperatures. One can include the FF deformations if needed, see Ref. [18], but I neglect this aspect here, as this is less relevant for I_{rel} . This distribution also favors slightly large relative orbital angular momenta (with an average of $\langle \phi^{LH} \rangle = 0.60$ and standard deviation 0.26), thus in agreement with Ref. [22] and the present analysis, and in disagreement with the results of Refs. [17] and [18]. The individual angular momenta distributions $\tilde{P}_1(S^L)$, $\tilde{P}_1(S^H)$ and $\tilde{P}_1(\Lambda)$ extracted by summing over the rest of the angular momenta, and which are shown in Fig. 3 along with the distributions from Eq. (9a) for $\tilde{P}_1(S^{L,H})$

$$\tilde{P}_1(S^F) = \sum_{\Lambda, f \neq F} \tilde{P}_3(S^F, S^f, \Lambda), \quad (28)$$

$$P(\Lambda) = \sum_{S^L, S^H} \tilde{P}_3(S^L, S^H, \Lambda), \quad (29)$$

are qualitatively similar, though not identical. The probability distributions $p(\phi^{LH})$ extracted using the triple distributions $\tilde{P}_3(S^L, S^H, \Lambda)$ from Eq. (12) and $\tilde{P}_3(S^L, S^H, \Lambda)$ from Eq. (27), as expected favor angles $\phi^{LH} > \pi/2$, see Fig. 4.

During the workshop [41] I realized that from the mi-

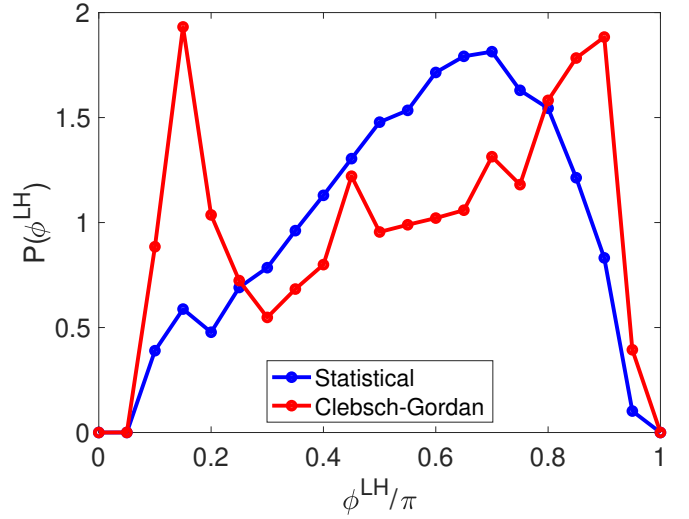


FIG. 4. The distribution $P(\phi^{LH})$ (normalized as in Fig. 2) obtained using the distributions $\tilde{P}_3(S^L, S^H, \Lambda)$ using Eq. (12) (Statistical) and $\tilde{P}_3(S^L, S^H, \Lambda)$ using Eq. (27) (Clebsch-Gordan). Both these distributions show a preference for angles $\phi^{LH} > \pi/2$ and both of them show a clear suppression of the FF intrinsic spins either parallel or antiparallel to each other. The statistical distribution here is slightly different from the one shown in Fig. 2, since in that case I used $P_1(\Lambda)$ from Eq. (9b) while here I used $P(\Lambda)$ from Eq. (29).

croscopic distribution $P_{\text{true}3}(S^L, S^H, \Lambda)$ from Ref. [22] as well as from the distributions $\tilde{P}_3(S^L, S^H, \Lambda)$ using Eq. (12) or $\tilde{P}_3(S^L, S^H, \Lambda)$ using Eq. (27) one can extract the double FF intrinsic spin distributions. E.g. in the case of $\tilde{P}_3(S^L, S^H, \Lambda)$

$$\tilde{P}_2(S^L, S^H) = \sum_{\Lambda} \tilde{P}_3(S^L, S^H, \Lambda) \approx \tilde{P}_1(S^L) \tilde{P}_1(S^H), \quad (30)$$

and similarly for the corresponding distributions $\tilde{P}_2(S^L, S^H)$ obtained from $\tilde{P}_3(S^L, S^H, \Lambda)$ and $P_2(S^L, S^H)$ obtained from $P_{\text{true}3}(S^L, S^H, \Lambda)$. This proves that the primordial FF intrinsic spins are essentially statistically independent before the emission of neutrons and statistical γ -rays, in complete agreement with the experimental observation of Wilson *et al.* [19], iff the orbital angular momentum is not recorded. Randrup and Vogt [18] make a similar claim, which follows directly from the assumed form of the FF rotational energy, see Eq. (22). The fact that $\tilde{P}_2(S^L, S^H) \approx \tilde{P}_1(S^L) \tilde{P}_1(S^H)$ (and the corresponding relations in the case of other triple distributions) appears to follow simply from general arguments, merely from the conservation of total angular momentum $|\langle (\mathbf{S}^L + \mathbf{S}^H + \mathbf{\Lambda})^2 \rangle = 0$ in case of spontaneous fission, with the expected (small) corrections in the case of fission induced by slow neutrons.

The actual spin distribution $P_{\text{true}3}(S^L, S^H, \Lambda)$ obtained in TDDFT simulations has a rather complicated

structure [22]. In Ref. [22] it was shown that

$$\sum_{S^L, S^H, \Lambda} |\mathcal{N}\hat{P}_1(\Lambda)\hat{P}_1(S^L)\hat{P}_1(S^H)\Delta - P_{\text{true}3}(S^L, S^H, \Lambda)| = 0.35, \quad (31)$$

where

$$\hat{P}_1(S^F) = \sum_{\Lambda, f \neq F} P_{\text{true}3}(S^F, S^f, \Lambda), \quad (32)$$

$$\hat{P}_1(\Lambda) = \sum_{S^L, S^H} P_{\text{true}3}(S^L, S^H, \Lambda). \quad (33)$$

The distributions $P_1(S^F)$ used to construct $\bar{P}_3(S^L, S^H, \Lambda)$ and $\tilde{P}_3(S^L, S^H, \Lambda)$ are slightly different from the distributions $\bar{P}_1(S^F)$ and $\tilde{P}_1(S^F)$ respectively, see Fig. 3. In the case of $\bar{P}_3(S^L, S^H, \Lambda)$

$$\sum_{S^L, S^H, \Lambda} |\mathcal{N}P_1(\Lambda)P_1(S^L)P_1(S^H)\Delta - \bar{P}_3(S^L, S^H, \Lambda)| \equiv 0 \quad (34)$$

by construction. Using Thomas Dossing's recent suggestion for $\tilde{P}_3(S^L, S^H, \Lambda)$ and the corresponding $\tilde{P}_1(S^L, S^H)$ and $P(\Lambda)$ one obtains

$$\sum_{S^L, S^H, \Lambda} |\mathcal{N}P(\Lambda)\tilde{P}_1(S^L)\tilde{P}_1(S^H)\Delta - \tilde{P}_3(S^L, S^H, \Lambda)| = 0.97. \quad (35)$$

In the case of $\bar{P}_3(S^L, S^H, \Lambda)$ I obtain

$$\sum_{S^L, S^H, \Lambda} |\mathcal{N}\bar{P}_1(\Lambda)\bar{P}_1(S^L)\bar{P}_1(S^H)\Delta - \bar{P}_3(S^L, S^H, \Lambda)| = 0.28, \quad (36)$$

thus closer to the case of the microscopic distribution. In this case $\bar{P}_1(S^L, S^H)$ and $\bar{P}_1(\Lambda)$ are obtained from $\bar{P}_3(S^L, S^H, \Lambda)$ by summing over the other two angular momenta. The main difference between the distribution suggested by Dossing and the one suggested here and the microscopic distribution as well, is the weight with which each configuration (S^L, S^H, Λ) is accounted for when constructing the corresponding correlated triple distributions. In the case of Dossing's distribution this weight is $\propto [C_{S^L, 0, S^H, 0}^{\Lambda, 0}]^2 / (2\Lambda + 1)$ vs 1 in the other cases. Moreover, Dossing's distribution allows only even values of $S^L + S^H + \Lambda$ [45], which is a rather strong restriction, considering that the FFs emerge highly excited.

An information theory characterization of the distributions discussed in this work is through the Shannon measure of the uncertainty, defined for an arbitrary probability distribution as $H = -\sum_X [P(X) \log_2 P(X)]$, where $P(X)$ is any probability distribution for a random variable X . The model distributions $\bar{P}_3(S^L, S^H, \Lambda)$ and $\mathcal{N}\bar{P}_1(\Lambda)\bar{P}_1(S^L)\bar{P}_1(S^H)\Delta$ introduced here have the corresponding uncertainties 12.47 and 12.43 respectively,

thus providing a comparable amount of uncertainty or information, see Eq. (36) and Figs. 2 and 4. At the same time, the amount of uncertainty corresponding to the distributions obtained following Dossing's suggestion, $\tilde{P}_3(S^L, S^H, \Lambda)$ and $\mathcal{N}\tilde{P}_1(\Lambda)\tilde{P}_1(S^L)\tilde{P}_1(S^H)\Delta$, are 10.71 and 11.45 respectively, which shows that the former has more information, in agreement with the Fig. 4, while the latter has more uncertainty. At the same time, as expected, both probability distributions obtained following Dossing's suggestion have more information, and thus less uncertainty. Using the microscopic distribution [22] $P_{\text{true}3}(S^L, S^H, \Lambda)$ and $\mathcal{N}\hat{P}_1(\Lambda)\hat{P}_1(S^L)\hat{P}_1(S^H)\Delta$ one obtains 12.94 and 12.54 in the case of the SeaLL1 nuclear energy density functional and 12.57 and 11.99 in the case of SkM* respectively.

The probability distribution $p(\phi^{LH})$ however appear to be less sensitive to finer details of the full distributions $P_{\text{true}3}(S^L, S^H, \Lambda)$ from Ref. [22], $\bar{P}_3(S^L, S^H, \Lambda)$ and $\tilde{P}_3(S^L, S^H, \Lambda)$, before and after the prompt neutron and statistical γ -rays emission, and it remains a challenge, particularly experimentally, to single out the potential observables, which can reveal them.

III. CONCLUSIONS

I have presented rather general arguments, not involving any specific properties of the nuclear interactions, that in a process where a system with a initial spin $S_0^\pi = 0^+$ decays into two fragments their intrinsic spins form an angle very close to $2\pi/3$ with a significant dispersion, a feature which one should typically expect in nuclear spontaneous fission in particular. The present conclusions agree with the parameter and assumption free independent microscopic calculations performed in Ref. [22]. Then, when a nucleus with a very small initial spin $\mathbf{S}_0 \approx \mathbf{0}$ fissions, the distribution of the intrinsic FF spins is determined mainly by statistical factors, namely by the rather large number of allowed final values of FF intrinsic spins. The range of the allowed FF intrinsic spins, in particular their distribution, is controlled by their intrinsic deformations [17, 18, 20–23]. In this respect the FF intrinsic spin distributions and their correlations are controlled mostly by the large final phase space allowed, as in case of many other types of decays, where the allowed phase space, in particular because the fraction of the phase space volume corresponding to angles $\phi^{LH} > \pi/2$ is approximately 2/3 of the total allowed phase space volume.

Moreover, if one considers the reduced distributions of the FF intrinsic spins alone, when the relative orbital angular momentum Λ is not recorded

$$\sum_{S^L, S^H} |P_2(S^L, S^H) - P_1(S^L)P_1(S^H)| = 0.08, 0.05 \text{ and } 0.02 \quad (37)$$

for the Dossing's distribution $\tilde{P}_3(S^L, S^H, \Lambda)$ [41], the

distribution $\overline{P}_3(S^L, S^H, \Lambda)$ discussed here, and for the microscopic distribution $P_{\text{true } 3}(S^L, S^H, \Lambda)$ evaluated in Ref. [22] respectively. The distribution $P_2(S^L, S^H)$ appears essentially uncorrelated, even before any prompt neutrons or statistical γ 's are emitted, thus in full agreement with the observation of Wilson *et al.* [19]. In this respect the system of three angular momenta is similar to the Borromean rings, which fall apart if one ring is cut off. The arguments presented here may apply also to heavy-ion collisions and atomic and molecular systems as well.

Acknowledgements

I thank Lee Sobotka for the willingness to have extensive discussions on these topics and for kindly agreeing to read a few initial drafts, which helped me sharpen my arguments, G. Scamps for discussions and reading of the manuscript, and J. Randrup for a very critical reading of the manuscript. The funding from the US DOE, Office of Science, Grant No. DE-FG02-97ER41014 and also the support provided in part by NNSA cooperative Agreement DE-NA0003841 is greatly appreciated. This research used resources of the Oak Ridge Leadership Computing Facility, which is a U.S. DOE Office of Science User Facility supported under Contract No. DE-AC05-00OR22725.

APPENDIX

It may be useful to consider the distribution $P(S^L, S^H, \phi^{LH})$ instead of the distribution $P_3(S^L, S^H, \Lambda)$. One can show that these two distributions are linked in the classical limit by the relation

$$P(S^L, S^H, \phi^{LH}) = P_3(S^L, S^H, \Lambda(\phi^{LH})) \frac{S^L S^H \sin(\phi^{LH})}{\Lambda(\phi^{LH})}$$

$$\Lambda(\phi^{LH}) = \sqrt{(S^L)^2 + (S^H)^2 + 2S^L S^H \cos(\phi^{LH})},$$

and as a result

$$P(\phi^{LH}) = \int dS^L dS^H P(S^L, S^H, \phi^{LH}) \propto \sin(\phi^{LH})$$

vanishes exactly at $\phi^{LH} = 0, \pi$, unless the integral

$$\int dS^L dS^H P_3(S^L, S^H, \Lambda(\phi^{LH})) \frac{S^L S^H}{\Lambda(\phi^{LH})}$$

diverges at least as $1/\sin(\phi^{LH})$. $\phi^{LH} = 0$ occurs on the upper face of the pyramid in Fig. 1, when $\Lambda = S^L + S^H$, and the two FF intrinsic spins are exactly parallel to each other. $\phi^{LH} = \pi$ occurs on the lateral faces of the pyramid, when $\Lambda = |S^L - S^H|$ and the two FF intrinsic spins are anti-parallel.

-
- [1] V. M. Strutinsky, "Angular Anisotropy of Gamma Quanta that Accompany Fission," *Sov. Phys. JETP* **10**, 613 (1960).
- [2] T. Ericson, "The statistical model and nuclear level densities," *Adv. Phys.* **9**, 425 (1960).
- [3] J. R. Huizenga and R. Vandenbosch, "Interpretation of Isomeric Cross-Section Ratios for (n, γ) and (γ, n) Reactions," *Phys. Rev.* **120**, 1305 (1960).
- [4] R. Vandenbosch and J. R. Huizenga, "Isomeric Cross-Section Ratios for Reactions Producing the Isomeric Pair $\text{Hg}^{197,197m}$," *Phys. Rev.* **120**, 1313 (1960).
- [5] J. R. Nix and W. J. Swiatecki, "Studies in the liquid-drop theory of nuclear fission," *Nucl. Phys.* **71**, 1 (1965).
- [6] J.O. Rasmussen, W. Nörenberg, and H.J. Mang, "A model for calculating the angular momentum distribution of fission fragments," *Nucl. Phys. A* **136**, 465 (1969).
- [7] J. B. Wilhelmy, E. Cheifetz, R. C. Jared, S. G. Thompson, H. R. Bowman, and J. O. Rasmussen, "Angular momentum of primary products formed in the spontaneous fission of ^{252}Cf ," *Phys. Rev. C* **5**, 2041–2060 (1972).
- [8] R. Vandenbosch and J.R. Huizenga, *Nuclear Fission* (Academic Press, New York, 1973).
- [9] L. G. Moretto and R. P. Schmitt, "Equilibrium statistical treatment of angular momenta associated with collective modes in fission and heavy-ion reactions," *Phys. Rev. C* **21**, 204 (1980).
- [10] T. Døssing and J. Randrup, "Dynamical evolution of angular momentum in damped nuclear reactions: (I). Accumulation of angular momentum by nucleon transfer," *Nucl. Phys. A* **433**, 215 (1985).
- [11] T. Døssing and J. Randrup, "Dynamical evolution of angular momentum in damped nuclear reactions: (II). Observation of angular momentum through sequential decay," *Nucl. Phys. A* **433**, 280 (1985).
- [12] L. G. Moretto, G. F. Peaslee, and G. J. Wozniak, "Angular-Momentum-Bearing Modes in Fission," *Nucl. Phys. A* **502**, 453c (1989).
- [13] C. Wagemans, ed., *The Nuclear Fission Process* (CRS Press, Boca Raton, 1991).
- [14] I. Stetcu, P. Talou, T. Kawano, and M. Jandel, "Isomer production ratios and the angular momentum distribution of fission fragments," *Phys. Rev. C* **88**, 044603 (2013).
- [15] B. Becker, P. Talou, T. Kawano, Y. Danon, and I. Stetcu, "Monte Carlo Hauser-Feshbach predictions of prompt fission γ rays: Application to $n_{\text{th}} + ^{235}\text{U}$, $n_{\text{th}} + ^{239}\text{Pu}$, and ^{252}Cf (sf)," *Phys. Rev. C* **87**, 014617 (2013).
- [16] J. Randrup and R. Vogt, "Refined treatment of angular momentum in the event-by-event fission model freya," *Phys. Rev. C* **89**, 044601 (2014).
- [17] R. Vogt and J. Randrup, "Angular momentum effects in fission," *Phys. Rev. C* **103**, 014610 (2021).
- [18] J. Randrup and R. Vogt, "Generation of Fragment Angular Momentum in Fission," *Phys. Rev. Lett.* **127**, 062502 (2021).
- [19] J. N. Wilson, D. Thisse, M. Lebois, N. Jovancevic, D. Gjestvang, R. Canavan, M. Rudigier, D. Etasse, R-B. Gerst, L. Gaudefroy, E. Adamska, P. Adsley, A. Al-

- gora, M. Babo, K. Belvedere, J. Benito, G. Benzoni, A. Blazhev, A. Boso, S. Bottoni, M. Bunce, R. Chakma, N. Cieplicka-Orynczak, S. Courtin, M. L. Cortes, P. Davies, C. Delafosse, M. Fallot, B. Fornal, L. Fraile, A. Gottardo, V. Guadilla, G. Hafner, K. Hauschild, M. Heine, C. Henrich, I. Homm, F. Ibrahim, L. W. Iskra, P. Ivanov, S. Jazrawi, A. Korgul, P. Koseoglou, T. Kroll, T. Kurtukian-Nieto, L. Le Meur, S. Leoni, J. Ljungvall, A. Lopez-Martens, R. Lozeva, I. Matea, K. Miernik, J. Nemer, S. Oberstedt, W. Paulsen, M. Piersa, Y. Popovitch, C. Porzio, L. Qi, D. Ralet, P. H. Regan, K. Rezyunkina, V. Sanchez-Tembleque, S. Siem, C. Schmitt, P. A. Soderstrom, C. Surder, G. Tocabens, V. Vedia, D. Verney, N. Warr, B. Wasilewska, J. Wiederhold, M. Yavahchova, F. Zeiser, and S. Ziliani, “Angular momentum generation in nuclear fission,” *Nature* **590**, 566 (2021).
- [20] A. Bulgac, I. Abdurrahman, S. Jin, K. Godbey, N. Schunck, and I. Stetcu, “Fission fragment intrinsic spins and their correlations,” *Phys. Rev. Lett.* **126**, 142502 (2021).
- [21] P. Marević, N. Schunck, J. Randrup, and R. Vogt, “Angular momentum of fission fragments from microscopic theory,” *Phys. Rev. C* **104**, L021601 (2021).
- [22] A. Bulgac, I. Abdurrahman, K. Godbey, and I. Stetcu, “Fragment Intrinsic Spins and Fragments’ Relative Orbital Angular Momentum in Nuclear Fission,” *Phys. Rev. Lett.* **128**, 022501 (2022).
- [23] I. Stetcu, A. E. Lovell, P. Talou, T. Kawano, S. Marin, S. A. Pozzi, and A. Bulgac, “Angular momentum removal by neutron and γ -ray emissions during fission fragment decays,” *Phys. Rev. Lett.* **127**, 222502 (2021).
- [24] J. Randrup, “Theory of transfer-induced transport in nuclear collisions,” *Nuclear Physics A* **327**, 490–516 (1979).
- [25] J. Randrup, “Transport of angular momentum in damped nuclear reactions,” *Nuclear Physics A* **383**, 468–508 (1982).
- [26] W. Hauser and H. Feshbach, “The inelastic scattering of neutrons,” *Phys. Rev.* **87**, 366 (1952).
- [27] S. Jin, K. J. Roche, I. Stetcu, I. Abdurrahman, and A. Bulgac, “The LISE package: solvers for static and time-dependent superfluid local density approximation equations in three dimensions, accepted in Comp. Phys. Comm.” *Comput. Phys. Commun.* **269**, 108130 (2021).
- [28] A. Bulgac, P. Magierski, K. J. Roche, and I. Stetcu, “Induced Fission of ^{240}Pu within a Real-Time Microscopic Framework,” *Phys. Rev. Lett.* **116**, 122504 (2016).
- [29] A. Bulgac, S. Jin, K. J. Roche, N. Schunck, and I. Stetcu, “Fission dynamics of ^{240}Pu from saddle to scission and beyond,” *Phys. Rev. C* **100**, 034615 (2019).
- [30] A. Bulgac, S. Jin, and I. Stetcu, “Nuclear Fission Dynamics: Past, Present, Needs, and Future,” *Frontiers in Physics* **8**, 63 (2020).
- [31] G. Salvioni, J. Dobaczewski, C. Barbieri, G. Carlsson, A. Idini, and A. Pastore, “Model nuclear energy density functionals derived from ab initio calculations,” *J. Phys. G: Nucl. Part. Phys.* **47**, 085107 (2020).
- [32] M. A. L. Marques, C. A. Ullrich, F. Nogueira, A. Rubio, K. Burke, and E. K. U. Gross, eds., *Time-Dependent Density Functional Theory*, Lecture Notes in Physics, Vol. 706 (Springer-Verlag, Berlin, 2006).
- [33] M. A. L. Marques, N. T. Maitra, F. M. S. Nogueira, E. K. U. Gross, and A. Rubio, eds., *Fundamentals of Time-Dependent Density Functional Theory*, Lecture Notes in Physics, Vol. 837 (Springer, Heidelberg, 2012).
- [34] O. Litaize, O. Serot, and L. Berge, “Fission modelling with FIFRELIN,” *Eur. Phys. Jour. A* **51**, 177 (2015).
- [35] J.M. Verbeke, J. Randrup, and R. Vogt, “Fission Reaction Event Yield Algorithm FREYA 2.0.2,” *Computer Physics Communications* **222**, 263–266 (2018).
- [36] P. Talou, I. Stetcu, P. Jaffke, M.E. Rising, A.E. Lovell, and T. Kawano, “Fission Fragment Decay Simulations with the CGMF Code,” *Comput. Phys. Commun.* **269**, 108087 (2021).
- [37] K.-H. Schmidt, B. Jurado, C. Amouroux, and C. Schmitt, “General description of fission observables: Gef model code,” *Nuclear Data Sheets* **131**, 107 – 221 (2016).
- [38] K.-H. Schmidt and B. Jurado, “Review on the progress in nuclear fission - experimental methods and theoretical descriptions,” *Rep. Prog. Phys.* **81**, 106301 (2018).
- [39] A. Bulgac, “Fission-fragment excitation energy sharing beyond scission,” *Phys. Rev. C* **102**, 044609 (2020).
- [40] G. F. Bertsch, “Reorientation in newly formed fission fragments (2019),” [arXiv:1901.00928](https://arxiv.org/abs/1901.00928).
- [41] *Workshop on Fission Fragment Angular Momenta, Seattle, USA, June 21-24, (2022)*, <https://indico.in2p3.fr/event/26459/>.
- [42] H. A. Bethe, “An attempt to calculate the number of energy levels of a heavy nucleus,” *Phys. Rev.* **50**, 332–341 (1936).
- [43] R. E. Langer, “On the Connection Formulas and the Solutions of the Wave Equation,” *Phys. Rev.* **51**, 669 (1937).
- [44] A. Bulgac, C. Lewenkopf, and V. Miskrjukov, “Generalized local approximation to the exchange potential,” *Phys. Rev. B* **52**, 16476 (1995).
- [45] D. A. Varshalovich, A. N. Moskalev, and V. K. Khersonskii, *Quantum Theory of Angular Momentum* (World Scientific, Singapore, 1989).